7 Hybrid EEG-fTCD Brain-Computer Interfaces

¹Aya Khalaf, ¹Ervin Sejdic and ¹Murat Akcakaya
¹University of Pittsburgh

Abstract (*< 250 words* **)**
This chapter introduces two novel hybrid brain computer interfaces (BCIs) based on electroencephalography (EEG) and functional transcranial Doppler ultrasound (fTCD). Non-invasive BCIs based on EEG have become popular due to cost effectiveness, high temporal resolution and portability of EEG recording devices, and systems with successful laboratory outcomes have been designed. However, the performance of the EEG-based BCIs prevent them from a consistent use by the target population, which usually includes individuals with limited speech and physical abilities. Various neuroimaging modalities that measure different brain activities have been used with EEG to improve the speed and accuracy performance of the non-invasive BCIs. The two hybrid BCIs introduced in this chapter are developed as alternatives to the existing systems and they were shown to balance between speed and accuracy and outperform the existing hybrid BCIs. Both systems measure electrical brain activity as well as cerebral blood flow velocity using EEG and fTCD, respectively. For these two systems, two different visual presentation paradigms are used to induce simultaneous changes in EEG and fTCD. The visual stimuli in the first system includes two objects flickering with different frequencies instructing word generation (WG) and mental rotation (MR) tasks, and the presentation in the second system includes two arrows instructing left and right motor imagery (MI) cognitive tasks. Experimental results shows that the flickering MR/WG presentation outperforms the MI presentation by 10% accuracy for task versus task problem. However, the MI presentation outperforms the MR/WG one in terms of transmission rates.

7.1 Introduction

Brain-computer interface (BCI) systems are commonly developed to aid individuals with limited speech and physical abilities, and they enable means to bypass neuromuscular activity and to mentally control external devices that can compensate for speech and/or motor impairments (Wolpaw et al. 2002), (Nicolas-Alonso and Gomez-Gil 2012). Usage of such systems as novel rehabilitation and intervention techniques to restore the lost functionalities have also been demonstrated (Blank et al. 2014),(Fager et al. 2011). Non-invasive BCIs are usually used to avoid risks of surgical procedures needed for invasive BCIs (Nicolas-Alonso and Gomez-Gil 2012). Electroencephalography (EEG) which measures brain electrical activity is widely used to design non-invasive BCIs due to its high temporal resolution, portability, and low cost (Wolpaw et al. 2002),(Farwell and Donchin 1988). However, EEG is highly non-stationary and it has low signal-to-noise ratio (SNR) negatively affecting its performance (Akcakaya et al. 2014). In order to improve both the speed and accuracy performance, hybrid BCI systems have been developed (Amiri, Fazel-Rezai, and Asadpour 2013). One way to develop such hybrid BCI systems is to exploit multimodal signals, specifically supporting EEG with another modality that is measured simultaneously as the EEG (Pfurtscheller et al. 2010), (Muller-Putz et al. 2015).

Even though there are various modalities that are used to support EEG for hybrid BCI design such as functional near-infrared spectroscopy (fNIRS) (Coyle et al. 2004), functional magnetic resonance imaging (fMRI) (Weiskopf et al. 2004), and magnetoencephalography (MEG) (Mellinger et al. 2007), fNIRS is the most commonly used modality for hybrid BCI design. This is mainly because fMRI and MEG are not portable, and hybrid BCIs built based on these modalities can only operate efficiently in controlled laboratory environments (Allison, Wolpaw, and Wolpaw 2007). For instance, EEG and fNIRS modalities were used to design asynchronous hybrid BCI in which the BCI user does not need any cue to initiate communication with the machine (Buccino, Keles, and Omurtag 2016). In this study, EEG and fNIRS data were recorded in response to motor execution tasks. Motor imagery (MI) tasks were employed for development of an EEG-fNIRS BCI in which occurrence of MI was detected using fNIRS modality while MI type was identified using EEG modality (Koo et al. 2015). Moreover, many researchers exploited both motor execution and MI tasks to design hybrid EEG-fNIRS BCIs and it was found that the data from both modalities due to different tasks complement each other (Fazli et al. 2012)(Blokland et al. 2014). In another EEG-fNIRS study, 4 commands were decoded using mental arithmetic and motor execution tasks (Khan, Hong, and Hong 2014).

Despite its popularity, fNIRS has relatively slow target response and the infrared transmission is difficult through hair (Min, Marzelli, and Yoo 2010). In addition, the number of fNIRS sensors to be used is variable and depends on the application (Naseer and Hong 2015). To overcome these limitations, we introduced functional transcranial Doppler ultrasound (fTCD) as an alternative to fNIRS. In our previous study, we have shown that compared to fNIRS, fTCD has a faster response time and less setup complexity since it uses only 2 ultrasound sensors to measure the cerebral blood velocity; and a BCI that is based on fTCD only can achieve accuracies of approximately 80% and 60% for binary and 3-class classification of different cognitive tasks within observation period of around 5 s (Aya Khalaf et al. 2018). Therefore, we argue that fTCD response time is comparable to EEG and it is a viable candidate to support EEG in a real-time BCI design.

In this chapter, we introduce two EEG and fTCD-based hybrid BCI designs. These two designs rely on detecting simultaneously induced changes in EEG and fTCD through two different visual presentation paradigms. In the first system, a visual paradigm will induce changes in cerebral blood flow (measured by fTCD) through the presentations of two stimuli that instruct word generation (WG) and mental rotation (MR) tasks, respectively. Simultaneously, the above mentioned two stimuli are designed to flicker with different frequencies and they induce steady state visual evoked potential in EEG (Aya Khalaf, Sejdic, and Akcakaya 2018b). In the second system, the visual presentation paradigm includes two stimuli directing the users to perform left or right motor imagery (MI), and MI induces changes simultaneously in EEG and fTCD (Aya Khalaf, Sejdic, and Akcakaya 2018a). Both visual presentation paradigms include a fixation cross to represent the baseline, see Section 7.2 for the details of the visual paradigms. Healthy participants were recruited to test both systems experimentally. For both systems, features derived from the power spectrum for both EEG and fTCD signals were calculated to identify the significant frequency bands in EEG and fTCD signals. Mutual information and linear support vector machines (SVM) were employed for feature selection and classification.

7.2 Visual Presentation Paradigms

We introduce two visual presentation paradigms to simultaneously induce changes in EEG and fTCD. These two visual presentation paradigms are then used to develop two different hybrid EEG and fTCD-based BCIs.

7.2.1 Flickering MR/WG-based Paradigm

The visual presentation paradigm includes two tasks and a fixation cross that represents the baseline. The presented tasks have to be differentiated by both EEG and fTCD modalities in order to obtain a successful hybrid BCI system. It was shown that word generation (WG) induces higher blood flow velocity in left middle cerebral arteries (MCAs) while the mental rotation (MR) induces bilateral activation enabling different responses fTCD (Myrden et al. 2011). However, such tasks cannot be distinguished using the EEG. Therefore, they cannot be directly employed in a hybrid EEG-fTCD system design. To build an efficient hybrid BCI in which cognitive tasks can be differentiated using both brain activity sensing modalities, we propose to combine the WG and MR tasks with steady state evoked potential (SSVEP) paradigm such that WG and MR tasks include a flickering checkerboard texture as shown in Fig.1.a (A. Khalaf et al. 2017). SSVEP-based BCIs have been extensively investigated for communication and control purposes (Bin et al. 2009), (Lesenfants et al. 2014), (Y.-T. Wang et al. 2017). In such SSVEP systems, visual stimuli with different flickering frequencies are used to elicit temporally matching electrical oscillations in the visual cortex (M. Wang et al. 2015). To issue a command to control an external device using SSVEP BCI, the user has to focus his/her attention on one of the visual stimuli shown on the screen. Recently, several studies focused on designing techniques to enhance the recognition of stimuli corresponding to the elicited SSVEPs. For instance, a joint frequency-phase modulation method was introduced to improve the differentiation between SSVEPs due to different stimuli (Chen et al. 2015). Another study suggested a novel spatial filtering approach known as task-related component analysis (TRCA) to enhance SSVEP detection (Nakanishi et al. 2018). On the other hand, other researchers focused on optimizing the stimulus time to enhance the performance of SSVEP BCI speller using fixed and dynamic optimization approaches (E. Yin et al. 2015).

More specifically, in the developed presentation paradigm, the icons/visual stimuli that instruct the users to perform WG and MR tasks were textured with a flickering checkerboard pattern as seen in Fig.1.a to induce SSVEPs in EEG. For SSVEPs to be elicited, the flickering frequency of the stimuli has to be in the range from 7 to 60 Hz (Vanegas, Blangero, and Kelly 2013). In addition, it was found that flickering frequencies higher than 20 Hz elicit SSVEPs with low amplitudes (Vanegas, Blangero, and Kelly 2013). Based on this information, WG and MR stimuli flickered with frequencies of 7 and 17 Hz. In addition, the system included a third class which is a fixation cross that represents the baseline. For flickering WG, a randomly chosen letter flickers on the screen in order to instruct the user to silently generate words starting with that letter. Flickering MR task is represented on the screen by a pair of flickering 3D similar shapes rotated with different angles and the user is asked to mentally rotate the shapes to decide if they are identical or mirrored. These shapes were inspired from a database of 3D shapes constructed from cubes (Peters and Battista 2008). The tasks were designed using Blender computer graphics software. During each trial, a vertical arrow points randomly to one of the 3 tasks for duration of 10 s and the user has to focus on performing the mental task specified by that arrow.

In summary, using the proposed presentation scheme, flickering checkerboard-textured tasks will induce SSVEPs in the EEG corresponding to the flickering frequency of each task leading to different EEG responses while word generation and mental rotation will induce different cerebral blood flow in the two hemispheres of the brain, therefore, they will generate distinct fTCD responses. The baseline EEG and fTCD will be recorded when the participants are performing no mental activity (while looking at the red cross located at the center of the screen).

7.2.2 Motor Imagery-based Paradigm

Among the existing diverse EEG-based BCI categories, BCIs based on motor imagery have been intensively used in rehabilitation applications that seek assisting disabled individuals as well as restoring individual's physical and cognitive functions lost due to neural disorders (van Dokkum, Ward, and Laffont 2015). Motor imagery (MI) is the process of movement imagination without any actual muscle activation. It was found that the MI process activates the same brain regions activated during the actual physical movement (Schlögl et al. 2005). Therefore, during the rehabilitation process, patients with motor impairments practice MI process to activate the injured brain motor regions (Kai Keng Ang et al. 2010). Several studies were performed on both healthy participants and participants with physical and/or speech impairments to examine the feasibility of motor imagery for BCI applications (Schlögl et al. 2005), (Ang and Guan 2017), (LaFleur et al. 2013). Towards motor recovery after stroke, several motor imagery BCIs with robotic feedback were developed (Kai Keng Ang et al. 2010), (Blank et al. 2014). Such systems decode the motor imagery signals into robot assisted movements and it was shown that such systems yielded motor improvements.

It was found that the cerebral blood velocity in left and right middle cerebral arteries (MCAs) changes depending on whether the moving arm is the left or the right one (Matteis et al. 2006). Such findings suggest that fTCD might be promising for MI-based BCIs. Inspired by these findings as well as the results we achieved previously with fTCD as a candidate for real-time BCIs (Aya Khalaf et al. 2018), we developed MI-based hybrid BCI that uses both EEG and fTCD modalities (Aya Khalaf, Sejdic, and Akcakaya 2018a). Such a system acquires the electrical activity of the brain using the EEG and the vascular response of the brain using the fTCD.

In the MI-based presentation scheme, a basic motor imagery task is visualized while acquiring EEG and fTCD simultaneously. As seen in Fig. 1.b, the screen shows a horizontal arrow pointing to the right representing right arm MI and another horizontal arrow pointing to the left representing left arm MI as well as a fixation cross that represents the baseline. Each trial lasts for 10 s. During each trial, a vertical small arrow, shown in Fig. 1.b, points randomly to one of the 3 tasks for duration of 10 s and the user has to take rest if the vertical arrow points to the fixation cross or to imagine moving either left or right arm depending on which MI task is specified by the vertical arrow.
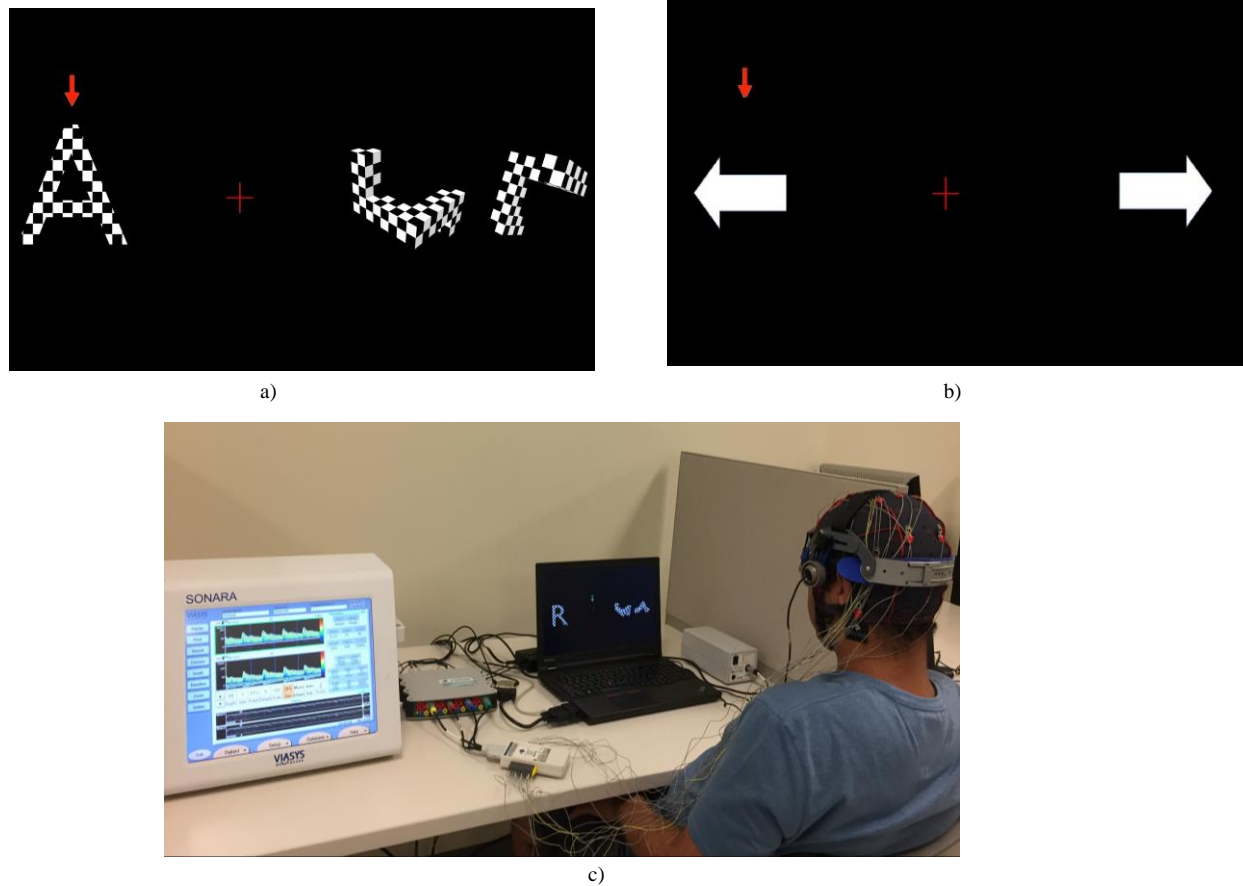
Fig. 1. Stimulus presentation for our flickering MR/WG (a) and the motor imagery EEG-fTCD BCI (b) as well as the hybrid system setup captured during one of the data collection sessions (c).

7.3 Methods

7.3.1 Data Acquisition

Sixteen electrodes were used to collect the EEG data. The electrodes were positioned over frontal, central, and parietal lobes at positions Fp1, Fp2, F3, F4, Fz, Fc1, Fc2, Cz, P1, P2, C1, C2, Cp3, Cp4, P5, and P6 according to the 10-20 system. Left mastoid was used as reference. Although SSVEPs give the strongest response over occipital area, we anticipated getting responses similar to those obtained from the occipital area using the electrodes mentioned above. Especially, we have electrodes on locations P5, and P6 which are close to the occipital area given that EEG is known to have low spatial resolution. A g.tec EEG system with a g. USBamp amplifier was used in this study. The amplifier included 16 24-bit simultaneously sampled channels with an internal digital signal filtering and processing unit and sampling rate up to 38.4 kHz. The data were digitized with a sampling rate of 256 samples/s and filtered by the amplifier's 8th order bandpass filter with corner frequencies of 2 and 62 Hz in addition to 4th order notch filter with corner frequencies of 58 and 62 Hz. Processed data were transferred from the amplifiers to a laptop via

USB 2.0.

A SONARA TCD system that utilizes two 2 MHz transducers was used to record fTCD signals. These transducers were placed on the left and right sides of the transtemporal window located above the zygomatic arch (Alexandrov et al. 2007). Since middle cerebral arteries (MCAs) provide approximately 80% of the brain with blood (Stroobant and Vingerhoets 2000), the fTCD depth was set to 50 mm which is the depth of the mid-point of the MCAs (Monsein et al. 1995). See Figure 1.c for the experimental setup.

7.3.2 Participants

21 healthy individuals participated in this study including 11 individuals (3 females and 8 males) with ages ranging from 25 to 32 years who participated in testing flickering MR/WG paradigm and 10 subjects (4 males and 6 females) with ages ranging from 23 to 32 who participated in testing MI paradigm. None of the participants had a history of migraines, concussions, strokes, heart murmurs, or other brain related injuries. The experiment lasted for approximately 1 hour and 15 min including the time required for the setup. All research procedures were approved by local Institutional Review Board (IRB) under the University of Pittsburgh IRB number of PRO16080475. Participants signed a written informed consent before starting the experiment. During the experiment, subjects were seated in a comfortable chair approximately 1 m away from the screen. Each participant attended one session. Each session included 150 trials. Each trial lasted 10 seconds and the trials are randomly but equally distributed across three conditions.

7.3.3 Feature Extraction and Fusion

Since each session contained 150 trials with 10 s duration per each, EEG and fTCD data corresponding to each observation were segmented. For each observation, the power spectrum was obtained for the corresponding 16 EEG segments as well as the corresponding 2 fTCD segments using Welch's power spectral density estimate (Welch 1967). Instead of using all the power spectrum values as features, the average of power spectrum values within a sliding window of specific width (in Hz) was considered as one feature. For the average power to be calculated for the next window, the original window was shifted by a value equal to its width so that there is no overlap between consecutive windows and so on. For EEG signals, the average power was calculated using a window of 2 Hz width. Since the fTCD signal has much higher bandwidth (≈2.5 KHz) compared to the EEG signals (≈40 Hz), and considering the need to reduce the number of features, a window of 50Hz width was used to reduce the fTCD power spectrum. The EEG/fTCD feature vector was formed by concatenating the features from all EEG/fTCD segments. The feature vectors of both EEG and fTCD signals were concatenated to form one single feature vector that represents each observation.

7.3.4 Feature Selection

Due to the high dimensionality of the EEG-fTCD feature vector (420 features), we applied a filter method for feature selection (Saeys, Inza, and Larranaga 2007). The main advantage of the filter methods compared to wrapper and embedded methods is the low computational complexity. Filtering is based on the mutual information (Hanchuan Peng, Fuhui Long, and Ding 2005). Specifically, in our approach, MI measures contribution of each feature towards taking a correct decision by assigning each feature a score based on its contribution. Higher MI score implies higher contribution of that feature towards correct classification. To calculate the mutual

information score, each feature is quantized adaptively such that the number of data samples is almost the same in each quantization bin so that quantization levels are equiprobable (Pohjalainen, Räsänen, and Kadioglu 2015). Mutual information score between the discretized feature value x and the class label y is given by (1).

$$MI = \sum_{x \in X} \sum_{y \in Y} p(x,y) log \left(\frac{p(x,y)}{p(x)p(y)} \right) \qquad (1)$$

In (1), x is the discretized feature value and y is the class label. In our approach, to determine the number of features to be used for each binary selection problem, the cumulative distribution function (CDF) of the mutual information scores was computed. We calculated CDF thresholds corresponding to probabilities ranging from 0.5 to 0.95 with 0.05 step in addition CDF thresholds corresponding to probabilities 0.98 and 0.99. For each CDF threshold, the features obtaining scores greater than or equal that threshold were selected. The performance measures including accuracy, sensitivity, and specificity corresponding to each CDF threshold are computed.

7.3.5 Classification and Performance Measures
Support vector machine (SVM) is used to perform the classification task (Chih-Wei Hsu and Chih-Jen Lin 2002). Basic SVM provides a discriminative approach that uses labeled data (supervised learning) to find the optimal hyperplane that gives the largest distance to the nearest training example. Since the BCI is intended to be used for real-time applications, the basic linear SVM is considered as the best choice especially if the BCI is designed to exploit an online adaptive update of the classifier parameters.

Six binary selection problems are formulated and classified using SVM. For the MI-based system, classification problems include right MI versus baseline, left MI versus baseline, right MI versus left MI; and for the Flickering MR/WG-based system the classification problems are MR versus baseline, WG versus baseline, and MR versus WG. For each participant, a subject-specific classifier is trained and tested using leave-one-out cross validation. Performance measures including accuracy and information transfer rate given by (2) are computed to evaluate the hybrid system (Obermaier et al. 2001).

$$B = log_2(N) + Plog_2(P) + (1-P)log_2\left(\frac{1-P}{N-1}\right) \qquad (2)$$

where N is the number of classes, P is the classification accuracy, and B is the data transmission rate per trial.

7.3.6 Evaluation of the Effectiveness of the Hybrid System

The nonparametric Wilcoxon signed rank test is used to assess the significance of the EEG-fTCD combination by statistically comparing the resultant performance measures with those obtained using EEG data only (Blair and Higgins 1980). Specifically, EEG-fTCD accuracy vector containing accuracies for all the participants as well as the corresponding EEG only accuracy vector for the same participants represented the 2 populations to be tested using Wilcoxon signed rank test. The test returns the p-value for the null hypothesis that assumes that the difference between the two populations follows a zero-median distribution.

7.3.7 Temporal Analysis to Identify Trial Length
An incremental window of 1 s initial width is used to calculate performance measures for each participant. The window width is increased by 1 s increment up to 10 s which is the trial length.

Performance measures are evaluated at each increment. The objective of this analysis to identify the optimum trial length that could be used to reduce the trial length and to improve the speed of the system. For each participant, the performance measures are computed as a function of time using 12 different CDF thresholds corresponding to probabilities ranging from 0.5 to 0.95 with 0.05 step as well as 0.98 and 0.99. These CDF thresholds are computed based on the CDF of mutual information scores reflecting the relevance of EEG and fTCD features within each binary selection problem, see also Section 7.3.4. Therefore, for every participant, 12 different profiles of performance measures across time are obtained. Considering subject-specific CDF thresholds, for each participant, all the accuracies at all CDF thresholds are considered and the maximum accuracy and the corresponding performance measures as well as the corresponding CDF threshold are used to represent that participant. Therefore, in subject-specific analysis, each subject might have different CDF threshold that corresponds to his/her maximum performance accuracy. Moreover, average of the maximum accuracy and the corresponding sensitivity, and specificity across all participants were obtained.

7.4 Results and Discussions

Tables 1 and 2 show the maximum accuracy achieved by each participant using the EEG-fTCD combination for MI-based and flickering MR/WG-based paradigms, respectively. In order to demonstrate the advantages of the hybrid system, classification accuracies are also calculated using EEG only and fTCD only with the same time interval (trial length) at which the EEG-fTCD combination gives the maximum accuracy as seen in Tables 1 and 2. Transmission rates corresponding to the accuracies and times listed in Tables 1 and 2 are also calculated for each binary problem using EEG data, fTCD data, and EEG-fTCD combination as seen in Fig. 2 and 3. Figure 2 and 3 present information transfer rates for MI-based and flickering MR/WG-based systems, respectively. The p-values representing the significance of the EEG-fTCD hybrid system are calculated by statistically comparing the EEG-fTCD accuracy/bit rate vector with the EEG only accuracy/bit rate vector for all the binary selection problems. Moreover, Table 3 compares the paradigms of the EEG and fTCD-based hybrid BCI with the state-of-the-art EEG and fNIRS-based hybrid BCIs.

As shown in Table 1, for right arm MI versus baseline problem, it was found that the EEG-fTCD combination achieved 88.33% average accuracy within 7.7s compared to 83.85% obtained by EEG only and 58.23% by fTCD only. The average accuracy difference between the hybrid combination and the EEG only was 4.48%. As seen in Fig. 2. (a), EEG-fTCD combination achieved higher bit rates compared to EEG only for all of the participants. On average, average transmission rate of 3.87 bits/min was obtained. Statistically, the EEG-fTCD combination achieved higher accuracy compared to EEG only for all the participants with a p-value of 0.002. As for left MI versus baseline, an average accuracy difference of 5.36% between the combination and EEG only was achieved with a p-value of 0.0078. For 8 out of 10 participants, EEG-fTCD scored higher accuracy compared to EEG only. EEG-fTCD scored 89.48% accuracy within 6.1s while EEG only scored 84.12% accuracy. As shown in Figure 2 (b), we obtained higher bit rates using EEG-fTCD combination compared to bit rates generated using EEG only and fTCD only. In addition, we achieved 6.02 bits/min average bit rate. Within 3.4 s, 82.38% average accuracy was achieved for right MI versus left MI problem using the EEG-fTCD combination and 77.62% using EEG only leading to a significant average accuracy difference of 4.76 % with 0.0195 p-value. The EEG-

fTCD combination scored higher accuracy for 8 out of 10 participants. On average, from Fig. 2. (c), 10.57 bits/min were achieved.

TABLE 1

Maximum accuracy (Acc) for each subject using hybrid system, EEG only, and fTCD only.

Sub_ID	Right arm MI vs baseline			Left arm MI vs baseline			right arm MI vs left arm MI		
	Acc_EEG	Acc_fTCD	Acc_Hybrid	Acc_EEG	Acc_fTCD	Acc_Hybrid	Acc_EEG	Acc_fTCD	Acc_Hybrid
1	91.67%	59.38%	**94.79%**	87.63%	65.98%	**97.94%**	82.86%	51.43%	**93.33%**
2	91.67%	61.46%	**92.71%**	91.75%	65.98%	**93.81%**	75.24%	38.10%	75.24%
3	81.25%	51.04%	**86.46%**	81.44%	51.55%	**93.81%**	71.43%	69.52%	**81.90%**
4	81.25%	55.21%	**87.50%**	78.35%	61.86%	**81.44%**	81.90%	53.33%	**85.71%**
5	87.50%	61.46%	**90.63%**	87.63%	53.61%	87.63%	78.10%	50.48%	**81.90%**
6	85.42%	56.25%	**86.46%**	74.23%	53.61%	**86.60%**	85.71%	42.86%	83.81%
7	80.21%	47.92%	**86.46%**	88.66%	54.64%	**90.72%**	71.43%	43.81%	**79.05%**
8	81.25%	69.79%	**91.67%**	85.57%	50.52%	**92.78%**	96.19%	50.00%	**97.14%**
9	71.88%	50.00%	**76.04%**	74.23%	48.45%	**79.38%**	70.48%	44.76%	**71.43%**
10	86.46%	69.79%	**90.63%**	91.75%	47.42%	90.72%	62.86%	66.67%	**74.29%**
Mean	83.85%	58.23%	**88.33%**	84.12%	55.36%	**89.48%**	77.62%	51.10%	**82.38%**

TABLE 2

Maximum accuracy (Acc) for each subject using hybrid system, EEG only, and fTCD only.

| Sub_ID	MR vs baseline			WG vs baseline			MR vs WG		
	Acc_EEG	Acc_fTCD	Acc_Hybrid	Acc_EEG	Acc_fTCD	Acc_Hybrid	Acc_EEG	Acc_fTCD	Acc_Hybrid
1	91.67%	50.00%	89.58%	82.47%	55.67%	**89.69%**	95.24%	51.43%	**99.05%**
2	84.38%	57.29%	**89.58%**	63.92%	43.30%	**67.01%**	82.86%	52.38%	**85.71%**
3	90.63%	56.25%	**93.75%**	73.20%	53.61%	**80.41%**	96.19%	73.33%	**97.14%**
4	83.33%	52.08%	**84.38%**	68.04%	42.27%	**76.29%**	84.76%	54.29%	**89.52%**
5	82.29%	46.88%	**88.54%**	68.04%	57.73%	**86.60%**	89.52%	63.81%	86.67%
6	90.63%	60.42%	**94.79%**	84.54%	53.61%	**89.69%**	90.48%	68.57%	**93.33%**
7	93.75%	39.58%	**94.79%**	94.85%	55.67%	**95.88%**	94.29%	57.14%	**96.19%**
8	88.54%	47.92%	**89.58%**	63.92%	50.00%	**68.04%**	88.57%	43.81%	**93.33%**
9	83.33%	50.00%	**86.46%**	78.35%	54.64%	78.35%	87.62%	47.62%	**88.57%**
10	58.33%	67.71%	**80.21%**	68.04%	62.89%	**75.26%**	91.43%	60.95%	91.43%
11	88.54%	38.54%	88.54%	80.41%	52.58%	**82.47%**	91.43%	52.38%	**95.24%**
Mean	85.04%	51.52%	**89.11%**	75.07%	52.91%	**80.88%**	90.22%	56.88%	**92.38%**
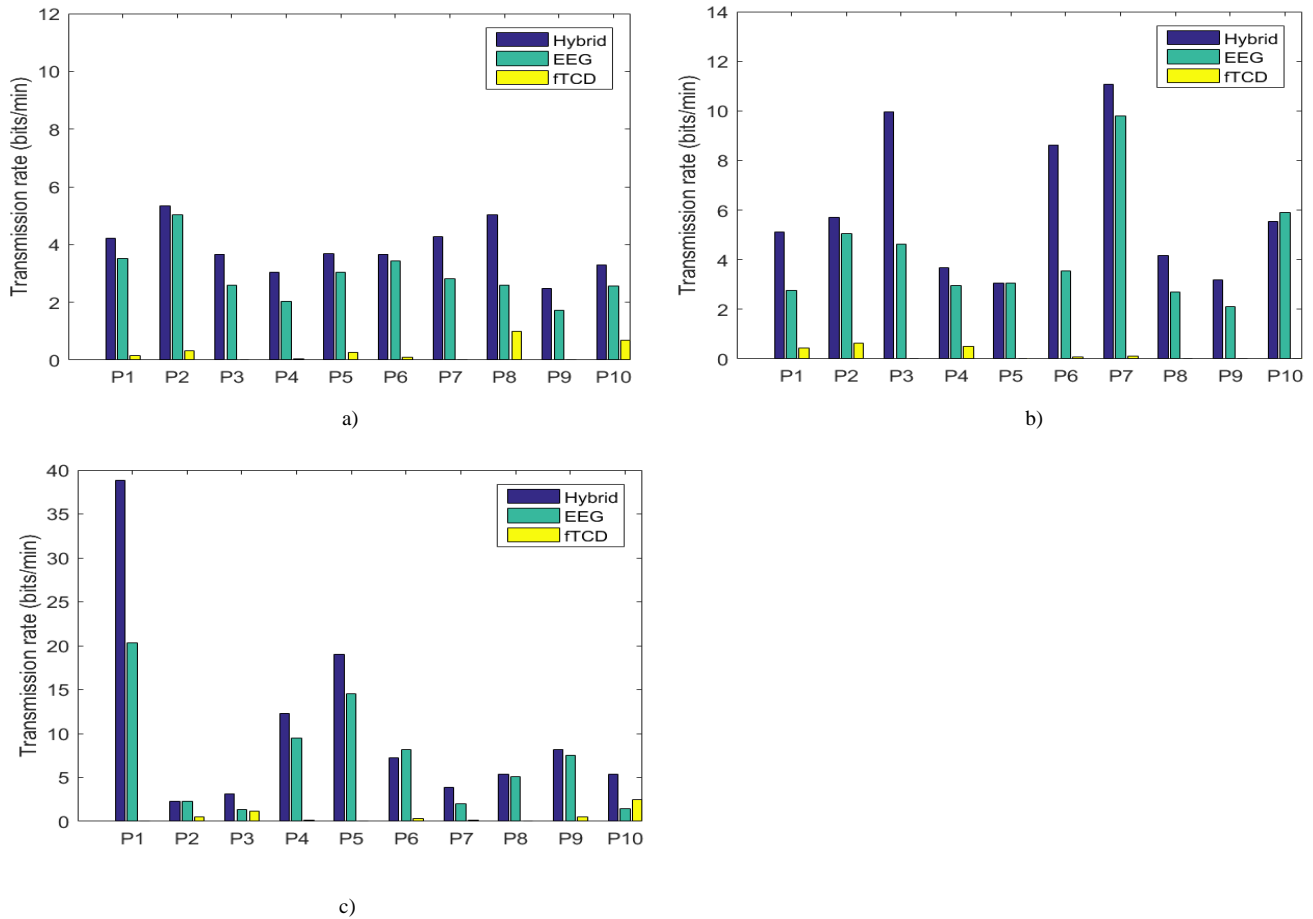
Fig. 2. Transmission rates for each participant (p) calculated using both EEG and fTCD, EEG only, and fTCD only for right arm MI vs baseline (a) left arm MI vs baseline problem (b) and right MI vs left MI (c).

EEG-fTCD combination achieved 89.11% average accuracy in approximately 7.73 s for MR versus baseline problem as seen in Table 2. The combination outperformed EEG only by an average accuracy difference of 4.06%. The EEG-fTCD combination scored higher accuracies than EEG only for 9 out of 11 participants. Performance measures obtained using fTCD only were nonsignificant. However, fTCD boosted the overall performance when it was combined with the EEG. In particular, the combination was proved to be significant compared to EEG only with a p-value of 0.0156. In terms of transmission rates, as shown in Fig.3, for most of the participants, the combination achieved higher bit rates compared to EEG only. Average bit rate of 4.39 bits/min was achieved. Considering WG versus baseline problem, as seen in Table 2, average accuracy difference of 5.81% between the EEG-fTCD combination and EEG only was achieved. Specifically, the combination achieved 80.88% average accuracy in 5.64 s while EEG only obtained 75.07%. The EEG-fTCD combination scored higher accuracies for 10 out of 11 participants using subject-specific thresholds. The hybrid system was shown to provide a significant accuracy improvement compared to EEG only with a p-value of 0.012. The EEG-fTCD combination achieved higher bit rates than EEG only for most of the participants as seen in Fig. 3. (b). Subject-specific thresholds achieved average bit rate of 3.92 bits/min. For MR vs WG problem, EEG-fTCD combination obtained 92.38% average accuracy in 7.82 s while EEG only got 90.22%.

The hybrid combination achieved higher accuracies for 9 out of 11 participants. Moreover, the hybrid combination was shown to be significant with p-value of 0.0078. Bit rates obtained using the EEG-fTCD combination were higher for most of the participants compared to those obtained using EEG as shown in Fig.3. (c). Average bit rate of 5.07 bits/min was obtained.
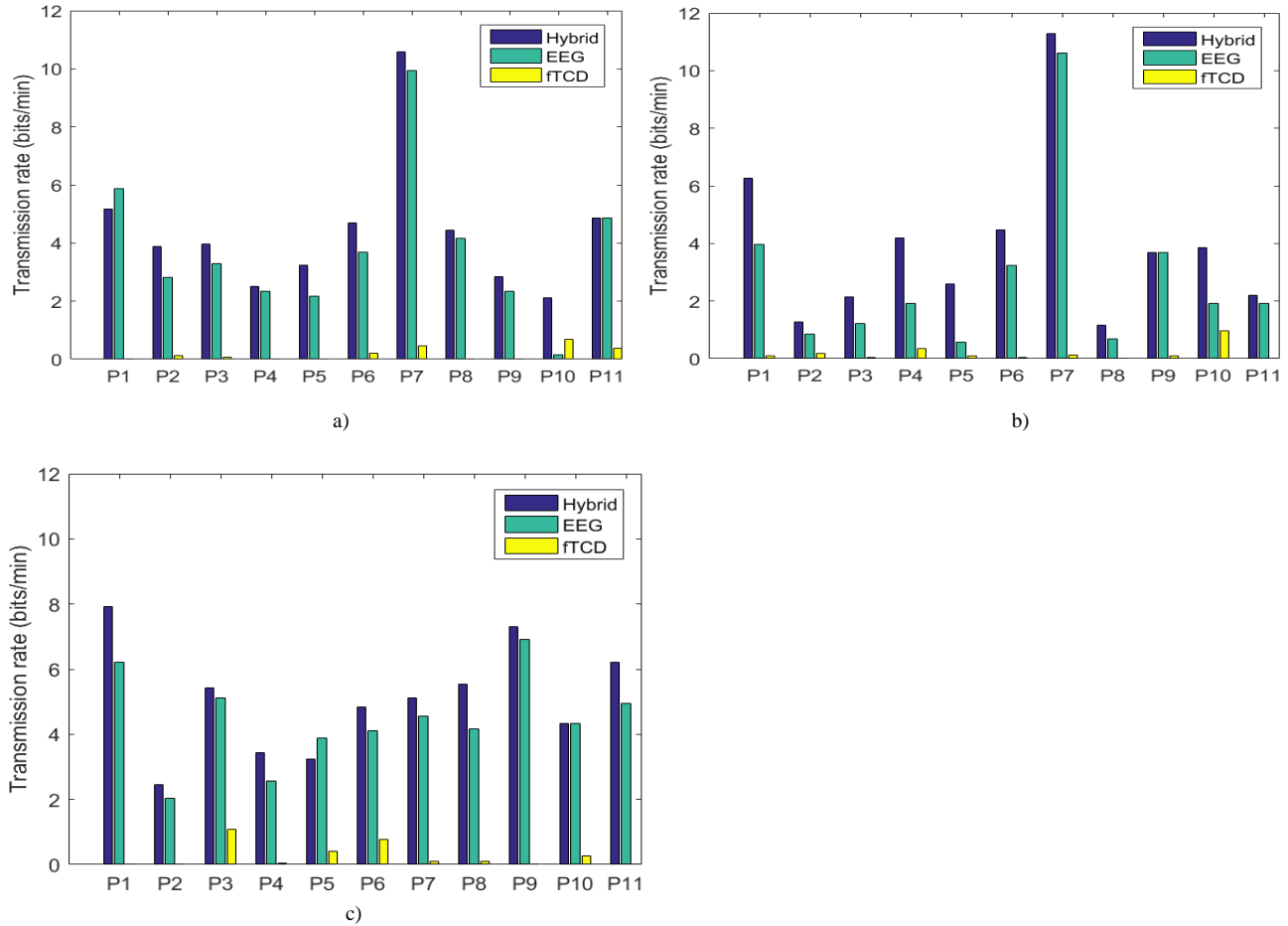

Fig. 3. Transmission rates for each participant (p) calculated using both EEG and fTCD, EEG only, and fTCD only for MR vs baseline (a) WG vs baseline problem (b) and MR vs WG (c).

Considering the MI visual presentation, by Inspecting the selected significant features across all participants for the right arm MI versus left arm MI problem, it was found that, across all electrodes, the EEG average power spectrum values at frequencies up to 2 Hz (delta frequency band) are the most common selected features across participants. Moreover, it was found that the common selected features belonging to theta (5-8 Hz) and mu (8–13 Hz) bands are coming from electrodes Fp1, Fp2, F3, and F4 while the common features belonging to beta (16–28 Hz) band are associated with electrodes C1, C2, Cp3, Cp4, P5, and P6. As for the fTCD, the common significant features were found at frequency bands 550-600, 2000-2050 and 2150-2200 Hz for the right fTCD channel and at frequency band 2050-2100 Hz for the left fTCD channel.

As for the flickering MR/WG visual presentation, through investigation of the common EEG and fTCD significant features across all participants for the classification problem that yielded the highest accuracy (WG versus MR), as expected, the top common EEG power spectrum features were found approximately around the 1st, 2nd, and 3rd harmonics of the 7 Hz and around 1st and 2nd harmonics of the 17 Hz. Considering the fTCD features, the most common selected significant power spectrum features were found at frequency bands of 0-50, 1200-1250, and 1350-1400 for the left fTCD channel and at frequency bands of 0-100, 300-350, and 1950-2000 Hz for the right fTCD channel.

In Table 3, we compared the proposed hybrid BCI with the state of the art EEG-fNIRS hybrid BCIs (Fazli et al. 2012), (Blokland et al. 2014), (Khan, Hong, and Hong 2014), (Putze et al. 2014), (X. Yin et al. 2015), (Koo et al. 2015), (Buccino, Keles, and Omurtag 2016), (Shin et al. 2017) . Accuracies of the above listed 6 binary selection problems are listed in Table 3. Comparisons were performed in terms of trial length and accuracy. For the EEG and fTCD-based hybrid BCI, comparing the MI-based presentation paradigm to the flickering MR/WG paradigm, we observe that the latter achieved an average of 10% increase in accuracy. However, the hybrid system based on MR/WG paradigm was slower since it required an average time of 6.36 sec to achieve 92.38% accuracy while the system based on MI paradigm required only 3.5 sec on average to achieve 82.38% accuracy.   In line with the differences in speed, flickering MR/WG presentation achieved maximum bit rate of 5.6 bits/min while MI visual presentation obtained 10.57 bits/min. On the other hand, right/left arm MI versus baseline achieved higher accuracies compared to right arm versus left arm MI. In contrast, it was found that MR/WG versus baseline problems achieved lower accuracies compared to MR versus WG problem. Since the location of the baseline cross is very close to the flickering MR and WG tasks as seen in Fig.1, the flickering affected the subject attention even during focusing at the baseline cross and thus caused reduction in accuracy for MR/WG versus baseline problems.

TABLE 3

Comparison between the proposed hybrid system and the state-of-the-art hybrid BCIs.

Method	BCI Type	Accuracy	Trial length (s)	
			Task	Baseline/rest
(Fazli et al. 2012)	EEG+fNIRS	83.20%	15	6/0
(Blokland et al. 2014)	EEG+fNIRS	79.00%	15	0/30±3
(Khan, Hong, and Hong 2014)	EEG+fNIRS	83.60%	10	0/5
(Putze et al. 2014)	EEG+fNIRS	94.70%	12.5±2.5	0/20 ±5
(X. Yin et al. 2015)	EEG+fNIRS	89.00%	10	0/21±1
(Koo et al. 2015)	EEG+NIRS	88.00%	15	0/60
(Buccino, Keles, and Omurtag 2016)	EEG+fNIRS	72.20%	6	6/0
(Buccino, Keles, and Omurtag 2016)	EEG+fNIRS	94.20%	6	6/0
(Shin et al. 2017)	EEG+fNIRS	88.20%	10	0/16±1
Proposed method (Left MI/baseline)	EEG+fTCD	88.33%	10	NA
Proposed method (Right MI/baseline)	EEG+fTCD	89.48%	10	NA
Proposed method (Right MI/left MI)	EEG+fTCD	82.38%	10	NA
Proposed method (MR/baseline)	EEG+fTCD	89.11%	10	NA
Proposed method (WG/baseline)	EEG+fTCD	80.88%	10	NA
Proposed method (MR/WG)	EEG+fTCD	92.38%	10	NA

*NA: Not applicable

Compared to the other BCIs listed in Table 3, in terms of trial length, the EEG and fTCD-based system has the shortest trial length of maximum 10 s. In addition, the proposed system is faster since it requires no baseline/rest period before/after each task. In terms of accuracy, the proposed hybrid BCI outperforms most of the methods in comparison. However, the systems introduced by Putze et al. (Putze et al. 2014) and Buccino et al. (Buccino, Keles, and Omurtag 2016) achieved higher accuracy compared to ours as they obtained 94.70% and 94.20% average accuracy respectively. Yet, these system are slower than our system since the one introduced by Putze et al. (Putze et al. 2014) requires at least 12.5 s as a task period and 20 s as a resting period while the one presented by Buccino et al. (Buccino, Keles, and Omurtag 2016) requires a baseline period of 6 s before starting each task.

Note here that despite the high accuracies obtained in a previous study with the fTCD data only (Aya Khalaf et al. 2018) , the presented hybrid system obtained lower accuracies with fTCD data only. It is well known that fTCD can differentiate imagery and analytical tasks since analytical tasks induce higher blood velocity in left MCAs while imagery tasks induce bilateral activation. However, for the MI-based system, both tasks are imagery tasks which makes the classification problem harder to solve. On the other hand, even though flickering MR/WG-based system utilizes both imagery and analytical tasks, the tasks were flickering to elicit SSVEPs. Such flickering reduced the concentration of each subject on the mental task to be performed. Moreover, in the previous study, a 15-min baseline period was recorded before starting the tasks to stabilize the cerebral blood flow. Also a resting period of 45 s was inserted between consecutive tasks. During the design of the two hybrid systems presented in this chapter, in order to improve the speed of the systems and also to reduce the trial length no baseline/rest periods were added to stabilize the cerebral blood. In fact, in the EEG and fTCD-based hybrid BCI systems, the baseline was shown at random times since it was designed as a task that resembles the condition in which the BCI user does not intend to produce a command.

7.6 Conclusions

In this chapter, we introduced two novel hybrid BCI systems that use EEG as the primary sensing modality to measure electrical brain activity and the fTCD as the secondary sensing modality to measure cerebral blood flow velocity. One of the systems was based on motor imagery to induce changes simultaneously in EEG and fTCD, while the other system simultaneously utilized mental rotation and word generation as stimuli for fTCD and flickering checkerboards to induce SSVEP in EEG. The experimental results that are obtained through the participation of 21 individuals were promising to show that the presented hybrid systems are feasible candidates for real-time BCI applications. Compared to the existing work on hybrid BCI that combines EEG with other modalities, the two hybrid systems show important progress towards making such systems real-world-worthy in terms of speed and accuracy. However, the systems still have limitations such that the temporal resolution of fTCD is lower than EEG resulting in longer trial lengths and decreasing the speed of the system. For example, such mismatch between the temporal resolution of these modalities can be minimized by introducing advanced analysis techniques for fTCD data to improve the obtained accuracy within the minimum possible task period. In particular, Wavelet analysis can be employed for fTCD analysis since it was used in a recent study (Aya Khalaf et al. 2018) to prove that fTCD is as a viable candidate for real-time BCIs and it achieved accuracies of approximately 80% and 60% for binary and 3-class BCIs within 3 and 5 s respectively. Further future directions could include

investigation of analysis techniques for both EEG and fTCD signals to increase accuracy and decrease trial length for the hybrid system so that the information transfer rate for the EEG-fTCD combination is increased. Morever, the generalization of the system across subjects could be explored using transfer learning techniques to decrease calibration requirements. On the other hand, based on the feedback from the BCI users, a bigger screen will be used to run the experiment to reduce the flickering effect on the subject's attention while focusing on the baseline cross. Moreover, the 25-min session will be divided into 2 sessions to reduce the user fatigue due to the flickering.

REFERENCES (APA styles)
Akcakaya, Murat et al. 2014. "Noninvasive Brain–Computer Interfaces for Augmentative and Alternative Communication." *IEEE Reviews in Biomedical Engineering* 7: 31–49. http://ieeexplore.ieee.org/document/6684304/ (February 12, 2019).
Aleem, Idris, and Tom Chau. 2013. "Towards a Hemodynamic BCI Using Transcranial Doppler without User-Specific Training Data." *Journal of Neural Engineering* 10(1): 016005. http://stacks.iop.org/1741-2552/10/i=1/a=016005?key=crossref.8bc75525330163c9501129b1248a6372 (September 7, 2016).
Alexandrov, Andrei V. et al. 2007. "Practice Standards for Transcranial Doppler Ultrasound: Part I-Test Performance." *Journal of Neuroimaging* 17(1): 11–18. http://doi.wiley.com/10.1111/j.1552-6569.2006.00088.x (August 7, 2016).
Allison, Brendan Z, Elizabeth Winter Wolpaw, and Jonathan R Wolpaw. 2007. "Brain-Computer Interface Systems: Progress and Prospects." *Expert review of medical devices* 4(4): 463–74. http://www.ncbi.nlm.nih.gov/pubmed/17605682 (August 28, 2016).
Amiri, Setare, Reza Fazel-Rezai, and Vahid Asadpour. 2013. "A Review of Hybrid Brain-Computer Interface Systems." *Advances in Human-Computer Interaction* 2013: 1–8. http://www.hindawi.com/journals/ahci/2013/187024/ (December 10, 2017).
Ang, Kai Keng, and Cuntai Guan. 2017. "EEG-Based Strategies to Detect Motor Imagery for Control and Rehabilitation." *IEEE Transactions on Neural Systems and Rehabilitation Engineering* 25(4): 392–401. http://ieeexplore.ieee.org/document/7802578/ (October 20, 2017).
Bin, Guangyu et al. 2009. "An Online Multi-Channel SSVEP-Based Brain–computer Interface Using a Canonical Correlation Analysis Method." *Journal of Neural Engineering* 6(4): 046002. http://stacks.iop.org/1741-2552/6/i=4/a=046002?key=crossref.501c725e9b2f8545feaf7401703ed8c1 (December 9, 2017).
Blair, R. Clifford, and James J. Higgins. 1980. "A Comparison of the Power of Wilcoxon's Rank-Sum Statistic to That of Student's T Statistic under Various Nonnormal Distributions." *Journal of Educational Statistics* 5(4): 309. http://www.jstor.org/stable/1164905?origin=crossref (August 8, 2016).
Blank, Amy A., James A. French, Ali Utku Pehlivan, and Marcia K. O'Malley. 2014. "Current Trends in Robot-Assisted Upper-Limb Stroke Rehabilitation: Promoting Patient Engagement in Therapy." *Current Physical Medicine and Rehabilitation Reports* 2(3): 184–

95. http://link.springer.com/10.1007/s40141-014-0056-z (October 20, 2017).

Blokland, Yvonne et al. 2014. "Combined EEG-fNIRS Decoding of Motor Attempt and Imagery for Brain Switch Control: An Offline Study in Patients With Tetraplegia." *IEEE Transactions on Neural Systems and Rehabilitation Engineering* 22(2): 222–29. http://www.ncbi.nlm.nih.gov/pubmed/24608682 (October 21, 2017).

Buccino, Alessio Paolo, Hasan Onur Keles, and Ahmet Omurtag. 2016. "Hybrid EEG-fNIRS Asynchronous Brain-Computer Interface for Multiple Motor Tasks" ed. Bin He. *PLOS ONE* 11(1): e0146610. http://dx.plos.org/10.1371/journal.pone.0146610 (October 21, 2017).

Chen, Xiaogang et al. 2015. "High-Speed Spelling with a Noninvasive Brain-Computer Interface." *Proceedings of the National Academy of Sciences of the United States of America* 112(44): E6058–67. http://www.ncbi.nlm.nih.gov/pubmed/26483479 (January 29, 2018).

Chih-Wei Hsu, Chih-Wei, and Chih-Jen Chih-Jen Lin. 2002. "A Comparison of Methods for Multiclass Support Vector Machines." *IEEE Transactions on Neural Networks* 13(2): 415–25. http://ieeexplore.ieee.org/lpdocs/epic03/wrapper.htm?arnumber=991427 (August 7, 2016).

Coyle, Shirley, Tomás Ward, Charles Markham, and Gary McDarby. 2004. "On the Suitability of near-Infrared (NIR) Systems for next-Generation Brain–computer Interfaces." *Physiological Measurement* 25(4): 815–22. http://stacks.iop.org/0967-3334/25/i=4/a=003?key=crossref.2b3bec58c1fb74ea68c7e4e57a6ac10d (September 6, 2016).

van Dokkum, L.E.H., T. Ward, and I. Laffont. 2015. "Brain Computer Interfaces for Neurorehabilitation – Its Current Status as a Rehabilitation Strategy Post-Stroke." *Annals of Physical and Rehabilitation Medicine* 58(1): 3–8. http://www.ncbi.nlm.nih.gov/pubmed/25614021 (October 21, 2017).

Fager, Susan et al. 2011. "Access Interface Strategies." *Assistive technology : the official journal of RESNA* 24(1): 25–33. http://www.ncbi.nlm.nih.gov/pubmed/22590797 (November 1, 2017).

Farwell, L A, and E Donchin. 1988. "Talking off the Top of Your Head: Toward a Mental Prosthesis Utilizing Event-Related Brain Potentials." *Electroencephalography and clinical neurophysiology* 70(6): 510–23. http://www.ncbi.nlm.nih.gov/pubmed/2461285 (November 1, 2017).

Fazli, Siamac et al. 2012. "Enhanced Performance by a Hybrid NIRS–EEG Brain Computer Interface." *NeuroImage* 59(1): 519–29. http://www.ncbi.nlm.nih.gov/pubmed/21840399 (October 21, 2017).

Hanchuan Peng, Fuhui Long, and C. Ding. 2005. "Feature Selection Based on Mutual Information Criteria of Max-Dependency, Max-Relevance, and Min-Redundancy." *IEEE Transactions on Pattern Analysis and Machine Intelligence* 27(8): 1226–38. http://ieeexplore.ieee.org/document/1453511/ (October 21, 2017).

Kai Keng Ang, Kai Keng et al. 2010. "Clinical Study of Neurorehabilitation in Stroke Using EEG-Based Motor Imagery Brain-Computer Interface with Robotic Feedback." In *2010 Annual International Conference of the IEEE Engineering in Medicine and Biology*, IEEE, 5549–52. http://www.ncbi.nlm.nih.gov/pubmed/21096475 (October 20, 2017).

Khalaf, A., M. Sybeldon, E. Sejdic, and M. Akcakaya. 2017. "An EEG and fTCD Based BCI for Control." In *Conference Record - Asilomar Conference on Signals, Systems and Computers*,.

Khalaf, Aya, Ervin Sejdic, and Murat Akcakaya. 2018a. "A Novel Motor Imagery Hybrid Brain Computer Interface Using EEG and Functional Transcranial Doppler Ultrasound." *Journal of Neuroscience Methods, Under Rev.*

———. 2018b. "Towards Optimal Visual Presentation Design for Hybrid EEG—fTCD Brain–computer Interfaces." *Journal of Neural Engineering* 15(5): 056019. http://stacks.iop.org/1741-2552/15/i=5/a=056019?key=crossref.48956e67c2a5bbd451b5d7f08db2ce08 (September 7, 2018).

Khalaf, Aya, Matthew Sybeldon, Ervin Sejdic, and Murat Akcakaya. 2018. "A Brain-Computer Interface Based on Functional Transcranial Doppler Ultrasound Using Wavelet Transform and Support Vector Machines." *Journal of Neuroscience Methods* 293: 174–82. http://www.sciencedirect.com/science/article/pii/S0165027017303515 (October 20, 2017).

Khan, M. Jawad, Melissa Jiyoun Hong, and Keum-Shik Hong. 2014. "Decoding of Four Movement Directions Using Hybrid NIRS-EEG Brain-Computer Interface." *Frontiers in Human Neuroscience* 8: 244. http://www.ncbi.nlm.nih.gov/pubmed/24808844 (January 28, 2018).

Koo, Bonkon et al. 2015. "A Hybrid NIRS-EEG System for Self-Paced Brain Computer Interface with Online Motor Imagery." *Journal of Neuroscience Methods* 244: 26–32. http://www.ncbi.nlm.nih.gov/pubmed/24797225 (October 21, 2017).

LaFleur, Karl et al. 2013. "Quadcopter Control in Three-Dimensional Space Using a Noninvasive Motor Imagery-Based Brain–computer Interface." *Journal of Neural Engineering* 10(4): 046003. http://stacks.iop.org/1741-2552/10/i=4/a=046003?key=crossref.ac48eeb233dce6b8bef5ccda9dae0dd2 (October 20, 2017).

Lesenfants, D et al. 2014. "An Independent SSVEP-Based Brain–computer Interface in Locked-in Syndrome." *Journal of Neural Engineering* 11(3): 035002. http://www.ncbi.nlm.nih.gov/pubmed/24838215 (November 1, 2017).

Matteis, M. et al. 2006. "Cerebral Blood Flow Velocity Changes during Meaningful and Meaningless Gestures - a Functional Transcranial Doppler Study." *European Journal of Neurology* 13(1): 24–29. http://www.ncbi.nlm.nih.gov/pubmed/16420390 (October 20, 2017).

Mellinger, Jürgen et al. 2007. "An MEG-Based Brain–computer Interface (BCI)." *NeuroImage* 36(3): 581–93.

Min, Byoung-Kyong, Matthew J. Marzelli, and Seung-Schik Yoo. 2010. "Neuroimaging-Based Approaches in the Brain–computer Interface." *Trends in Biotechnology* 28(11): 552–60. http://www.ncbi.nlm.nih.gov/pubmed/20810180 (October 21, 2017).

Monsein, Lee H. et al. 1995. "Validation of Transcranial Doppler Ultrasound with a Stereotactic Neurosurgical Technique." *Journal of Neurosurgery* 82(6): 972–75. http://thejns.org/doi/abs/10.3171/jns.1995.82.6.0972 (August 7, 2016).

Muller-Putz, Gernot et al. 2015. "Towards Noninvasive Hybrid Brain-Computer Interfaces: Framework, Practice, Clinical Application, and Beyond." *Proceedings of the IEEE* 103(6): 926–43. http://ieeexplore.ieee.org/document/7109824/ (October 21, 2017).

Myrden, Andrew J. B. et al. 2011. "A Brain-Computer Interface Based on Bilateral Transcranial Doppler Ultrasound" ed. Gennady Cymbalyuk. *PLoS ONE* 6(9): e24170. http://dx.plos.org/10.1371/journal.pone.0024170 (October 21, 2017).

Nakanishi, Masaki et al. 2018. "Enhancing Detection of SSVEPs for a High-Speed Brain Speller

Using Task-Related Component Analysis." *IEEE Transactions on Biomedical Engineering* 65(1): 104–12. http://ieeexplore.ieee.org/document/7904641/ (January 29, 2018).

Naseer, Noman, and Keum-Shik Hong. 2015. "fNIRS-Based Brain-Computer Interfaces: A Review." *Frontiers in human neuroscience* 9: 3. http://www.ncbi.nlm.nih.gov/pubmed/25674060 (January 29, 2018).

Nicolas-Alonso, Luis Fernando, and Jaime Gomez-Gil. 2012. "Brain Computer Interfaces, a Review." *Sensors (Basel, Switzerland)* 12(2): 1211–79. http://www.ncbi.nlm.nih.gov/pubmed/22438708 (October 20, 2017).

Obermaier, B., C. Neuper, C. Guger, and G. Pfurtscheller. 2001. "Information Transfer Rate in a Five-Classes Brain-Computer Interface." *IEEE Transactions on Neural Systems and Rehabilitation Engineering* 9(3): 283–88. http://ieeexplore.ieee.org/document/948456/ (January 24, 2018).

Peters, Michael, and Christian Battista. 2008. "Applications of Mental Rotation Figures of the Shepard and Metzler Type and Description of a Mental Rotation Stimulus Library." *Brain and Cognition* 66(3): 260–64.

Pfurtscheller, Gert et al. 2010. "The Hybrid BCI." *Frontiers in Neuroscience* 4: 3. http://journal.frontiersin.org/article/10.3389/fnpro.2010.00003/abstract (January 24, 2018).

Pohjalainen, Jouni, Okko Räsänen, and Serdar Kadioglu. 2015. "Feature Selection Methods and Their Combinations in High-Dimensional Classification of Speaker Likability, Intelligibility and Personality Traits." *Computer Speech & Language* 29(1): 145–71. http://linkinghub.elsevier.com/retrieve/pii/S0885230813001113 (December 9, 2017).

Putze, Felix et al. 2014. "Hybrid fNIRS-EEG Based Classification of Auditory and Visual Perception Processes." *Frontiers in neuroscience* 8: 373. http://www.ncbi.nlm.nih.gov/pubmed/25477777 (January 28, 2018).

Saeys, Y., I. Inza, and P. Larranaga. 2007. "A Review of Feature Selection Techniques in Bioinformatics." *Bioinformatics* 23(19): 2507–17. https://academic.oup.com/bioinformatics/article-lookup/doi/10.1093/bioinformatics/btm344 (October 31, 2017).

Schlögl, Alois, Felix Lee, Horst Bischof, and Gert Pfurtscheller. 2005. "Characterization of Four-Class Motor Imagery EEG Data for the BCI-Competition 2005." *Journal of Neural Engineering* 2(4): L14–22. http://stacks.iop.org/1741-2552/2/i=4/a=L02?key=crossref.b48710597fa273469a1d48e6b80b7177 (October 20, 2017).

Shin, Jaeyoung et al. 2017. "Evaluation of a Compact Hybrid Brain-Computer Interface System." *BioMed Research International* 2017: 1–11. https://www.hindawi.com/journals/bmri/2017/6820482/ (November 1, 2017).

Stroobant, N, and G Vingerhoets. 2000. "Transcranial Doppler Ultrasonography Monitoring of Cerebral Hemodynamics during Performance of Cognitive Tasks: A Review." *Neuropsychology review* 10(4): 213–31. http://www.ncbi.nlm.nih.gov/pubmed/11132101 (October 21, 2017).

Vanegas, M Isabel, Annabelle Blangero, and Simon P Kelly. 2013. "Exploiting Individual Primary Visual Cortex Geometry to Boost Steady State Visual Evoked Potentials." *Journal of neural engineering* 10(3): 036003. http://www.ncbi.nlm.nih.gov/pubmed/23548662 (January 28, 2018).

Wang, Minjue et al. 2015. "A New Hybrid BCI Paradigm Based on P300 and SSVEP." *Journal of Neuroscience Methods* 244: 16–25. http://www.ncbi.nlm.nih.gov/pubmed/24997343 (October 31, 2017).

Wang, Yu-Te et al. 2017. "An Online Brain-Computer Interface Based on SSVEPs Measured From Non-Hair-Bearing Areas." *IEEE Transactions on Neural Systems and Rehabilitation Engineering* 25(1): 14–21. http://ieeexplore.ieee.org/document/7480820/ (November 1, 2017).

Weiskopf, N. et al. 2004. "Principles of a Brain-Computer Interface (BCI) Based on Real-Time Functional Magnetic Resonance Imaging (fMRI)." *IEEE Transactions on Biomedical Engineering* 51(6): 966–70. http://ieeexplore.ieee.org/lpdocs/epic03/wrapper.htm?arnumber=1300789 (September 6, 2016).

Welch, P. 1967. "The Use of Fast Fourier Transform for the Estimation of Power Spectra: A Method Based on Time Averaging over Short, Modified Periodograms." *IEEE Transactions on Audio and Electroacoustics* 15(2): 70–73. http://ieeexplore.ieee.org/document/1161901/ (February 27, 2017).

Wolpaw, Jonathan R et al. 2002. "Brain-Computer Interfaces for Communication and Control." *Clinical neurophysiology : official journal of the International Federation of Clinical Neurophysiology* 113(6): 767–91. http://www.ncbi.nlm.nih.gov/pubmed/12048038 (October 31, 2017).

Yin, Erwei et al. 2015. "A Dynamically Optimized SSVEP Brain–Computer Interface (BCI) Speller." *IEEE Transactions on Biomedical Engineering* 62(6): 1447–56. http://www.ncbi.nlm.nih.gov/pubmed/24801483 (May 27, 2018).

Yin, Xuxian et al. 2015. "A Hybrid BCI Based on EEG and fNIRS Signals Improves the Performance of Decoding Motor Imagery of Both Force and Speed of Hand Clenching." *Journal of Neural Engineering* 12(3): 036004. http://stacks.iop.org/1741-2552/12/i=3/a=036004?key=crossref.fe66dac345d35e64effc9b537cbab91c (October 21, 2017).